Journal of Engineering and Technology

ISSN 2180-3811 eISSN 2289-814X https://jet.utem.edu.my/jet/index

NUMERICAL EVALUATION OF WALL POROSITY ON HYDROMAGNETIC SLIP FLOW DUE TO VARIABLE THERMAL CONDUCTIVITY

A. M. M. Hamza[1], D. Sani[1] and G. Ojemeri*[2]

[1]Department of Mathematics, Faculty of Physical and Computing Sciences, Usmanu Danfodiyo University, P. M. B. 2346, Sokoto.

[2] Department of Mathematics, College of Sciences, Federal University of Agriculture, P. M. B. 28, Zuru, Kebbi State.

**corresponding: godwinojemeri@gmail.com*

Article history:
Received Date: 16 February 2024
Revised Date: 12 September 2024
Accepted Date: 29 October 2024

Keywords:
Buoyancy force Parameter, Magnetohydrodynamics (MHD), Slip Flow, Suction/injection,

Abstract— In boundary layer control, especially in engineering, aerodynamics, space research, and medicine, suction/injection factors are very crucial. These advantages prompted our interest to dig further into the effect of wall porosity in industrial working fluids. Therefore, this paper analyses unsteady magnetized flow through an upstanding plate with the involvement of suction/injection flow and Navier slip flow due to the actions of variable buoyancy force and thermal conductivity distributions. The nonlinear partial differential equations for momentum and energy are modeled under the

Variable Thermal Conductivity, Wall Porosity	Boussinesq assumption using a semi implicit finite difference scheme, while the analytical results of the steady-state equations were calculated employing the regular perturbation technique. The solutions obtained were presented and discussed in detail using various line graphs. It is concluded that the slip flow parameter promotes fluid velocity, while the same effect occurs when the injection parameter is increased. However, a counter-feature can be observed: higher suction and magnetic parameters values lead to a drastic reduction in fluid movement respectively. The outcomes of this study would be helpful for controlling fluid flow in channels as well as aiding the addition and removal of reactants during chemical reactions.

I. Introduction

The study of electrically conductive liquids, including plasma, electrolytes, salt water, and liquid metals, is called magnetohydrodynamics (MHD). There are numerous technical and commercapplications for this type of liquid, including magnetic drug targeting, crystal formation, power generation, reactor cooling, and MHD sensors [1]. Hartmann and Lazarus [2] were the first to conduct an experimental study of modern MHD flow in laboratories. This research laid the groundwork for the creation of numerous MHD devices, including MHD pumps, MHD generators, brakes, flow meters, and geothermal powered energy extraction. Since then, many works have been published to investigate the impacts of MHD on free convection through various flow channels. To this end, Ojemeri and Onwubuya [3]

recently investigated the consequences of viscous dissipation and porosity effects on MHD free convection flow of an incompressible fluid traveling along a slit microchannel that is alternately heated and equipped with superhydrophobic slip and temperature conditions. In another related work, Onwubuya and Ojemeri [4] performed a comparative analysis of MHD mixed convection with thermal radiation factor in an upstanding porous channel using homotopy perturbation approach. Hamza et al. [5] explained the impact of hydromagnetic natural convection flow on a chemically reacting fluid affected by symmetric and asymmetric heating conditions using the homotopy perturbation technique. Jha et al. [6] echoed the significance of the buoyancy-induced magnetic field flow of a fluid in an upright channel having point or line heat generation or absorption at various channel positions. Jha et al. [7] were concerned with the Couette flow of a viscous fluid in free convection in an upward channel constructed between two infinitely vertically parallel porous plates in both steady-state and unsteady states. Hydromagnetic Casson nanofluidic flow for mass and heat transport through a stretching plate was studied by Saeed and Gul [8]. The consequences of cross-diffusion on non-Newtonian fluid flow over an extended range employing an unequal heat sink/source were researched by Reddy et al. [9]. The Fehlberg approach was employed in this analysis to get the answer to the modelled problem. The joint functions of fractional and non-uniform heat on the flow regime were investigated by the authors. The actions of heat absorption/generation and chemical reaction on the Maxwell hydromagnetic nanofluid flux were discussed by Sravanthi and Gorla [10]. The authors used the semi-analytical method and homotopy analysis method (HAM) to solve the formulated model in this problem by considering flow over an extended surface with exponential convection. The

significance of Soret on hydromagnetic heat and mass transfer flux across an upstanding porous plate flowing semi-infinitely, involving chemical reactions and heat generation, has been reported by Gurivireddy et al. [11]. Ojemeri et al. [12] deliberated on the hydromagnetic flux of an electrically conducting non-Newtonian liquid instigated by the radiative factor in an upright porous channel. References like [13-16] shed more light on this phenomenon.

Thermal conductivity is thought to be constant in certain previously published publications. However, it is well recognized that temperature fluctuations can drastically alter the fluid's physical characteristics. The fluctuation of thermal conductivity with temperature must be considered to correctly anticipate flow behavior and heat transfer rate. Thermal characteristics, in particular thermal diffusivity and conductivity are crucial bedrock material parameters that regulate heat transmission and temperature increases in the repository zone [17]. Variable thermophysical fluid characteristics are therefore crucial for improving fluid heat transmission. The heat transport system is noticeably impacted by temperature-dependent thermal conductivity and viscosity. Several published works on steady flow with varying thermal conductivity are available. Salawu et al. [18] took this into account when modeling the natural convection flow of a sliding upright channel, which is approximated by the Boussinesq approximation for the buoyancy force and variable thermal conductivity. They reported that a temperature difference in the device facilitates heat transfer and fluid flow. The consequence of temperature-dependent variable thermal conductivity in natural convection under the control of a uniform magnetic field has been investigated by Hamza et al. [19]. An isothermal upstanding plate is immersed in a thermally conductive liquid, and the impacts of different viscosities and thermal conductivities on the natural MHD convection across the

plate are studied by Pradip et al. [20]. Natural hydromagnetic flux with varying thermal conductivity across an inclined radiation-isothermal porous wall was a topic of discussion for Reddy [21]. Animasaun and Sandeep [22] investigated how the concentration of a nanofluid stream affects variable thermal conductivity and viscosity. Carreau cross fluids provoked by variable thermal radiation and thermal conductivity factors were solved by Salahuddin and Awais [23]. The magneto-hydrodynamic Carreau flow was investigated by Abbas et al. [24] utilizing the homotopy approach with variable fluid parameters. Khan et al. [25] used the Keller-Box approach to study a Carreau liquid surface with different thicknesses. The functions of thermal radiation and viscous dissipation on natural convective fluid were investigated by Nalivale et al. [26]. Carreau liquid with heat flux and thermal property affected by the radiation effect was proposed by Megahed et al. [27]. In their study on heat sources and sinks, Irfan et al. [28] generalized Fourier's law to be affected by the actions of different thermal conductivities in the Carreau liquid flow. Waqas et al. [29] emphasized the influence of different fluid parameters on the Carreau fluid in a stagnation point flow with mixed convection. Ewis [30] carefully studied the impacts of variable thermal conductivity, Darcy number, and Grashof number on heat transfer and free convection in viscoelastic fluids. In their article, Hamza et al. [31] echoed the significance of steady-state mixed convection along a microchannel whose plates are believed to be affected by momentum slip and energy jump effects. The implications of variable viscosity, thermal conductivity, and magnetic fields on convective free heat and mass transfer flux along a porous material influenced by uniform heat flux were studied by Borah and Hazarika [32]. They found that with increasing viscosity and thermal conductivity, the temperature decreased. Other works that investigated the applications of this concept include [33-36].

Suction and/or injection occurs when a plane surface or channel wall has pores or openings that allow fluid leakages. Studies such as Mishra et al. [37], Chaudhary and Jain [38] and Khalid et al. [39] exemplify the phenomena. Suction/injection plays a critical function in boundary layer regulation, especially in engineering, aerodynamics, space research, and medicine. These applications gained our curiosity to investigate the role of suction/injection in different types of fluids. To this end, Jha et al. [40] used the Laplace transform approach to study the impact of suction or injection on steady free convection in a vertical channel driven by point or line heat generation or absorption effects. In another investigation, Uwanta et al. [41] showed the influence of suction/injection on hydro-magnetic natural convection flow in vertical plates. It has been noticed that suction or injection can be used to control fluid flow in the channel. Jha et al. [42] investigated the effect of suction/injection on natural convection flow in transient magneto-hydrodynamics.

Moreover, Jha et al. [43] studied the effect of suction/injection on hydro-magnetic free convection flow. They discovered that increasing velocity lowers injection parameters as well. Suction parameters rise as shear stress increases. Kamis et al. [44] investigated heat transfer analysis in the blood fluid-based copper and alumina nano elements across an unsteady stretching sheet affected by suction/injection. Other works that provided some comprehensive insights into the impacts of unsteady magnetized hybrid nanofluid flow across a stretching or shrinking thin film with suction/injection effects can be found in references [45-48].

Processes such as heating, ventilation, and air conditioning (HVAC), antifreeze or heat exchange fluid flows in a nuclear reactor, and heat transfer composition have recently grown significantly to maximize efficiency. These developments have been made possible using

improved working fluids, novel channel walls with enhanced heat insulation features, or inventive geometric designs. Therefore, the study of fluid suction or injection flow is of crucial importance for medical sciences as well as technical applications such as the cooling and drying of paper and textiles and the extrusion of metals and polymers, to name a few. It is used for problems with blood circulation, blood flow, cancer treatment, aerodynamics, and other things. Hence, the motivation for this study. To study the analytical and numerical effects of suction and injection on the transient flow of a viscous and electrically conductive fluid having thermal properties and buoyancy under the influence of slip flow conditions, a novel mathematical model is developed in the present study as an extension of the work by Hamza et al. [19]. The displayed line graphs have been used to examine the consequences of important control parameters embedded in the flow configuration. In addition, when comparing the numerical solution and the steady-state solution over a longer period, a high level of agreement was shown, confirming the accuracy and precision of the current analysis.

II. Formulation of the Problem

Envisage the unsteady free convection flow of an electrically conducting fluid in the involvement of suction/injection, gliding flow, and a transversely applied magnetic field of intensity B_0, within two upstanding plates. It is initially thought that the liquid and the walls are at rest and have the same temperature T'm.

The temperature of the walls is immediately increased or decreased to T'_h or T'_c, respectively, at time $t' > 0$, so that $T'_h > T'_c$ holds, which is thereafter maintained to be constant. As shown in Figure 1, we have chosen a Cartesian coordinate system where the x-axis is vertical, and the y-axis is normal to it.

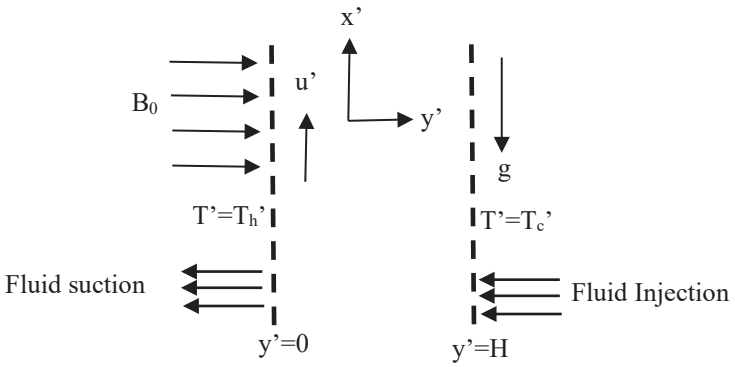

Figure 1: Schematic representation of the flow problem

The thermal conductivity (kf) of the liquid is thought to be to changing linearly with temperature in the form $kf = km\,[1 + \delta\,(T' - T'm)]$, see Elbarbary and Elgazery [49], where km is the free-flow heat of the liquid is conductivity and δ is a constant that varies with the properties of the fluid, with $\delta > 0$ for fluids namely water and air and $\delta < 0$ for fluids such as lubricating oils Elbarbary and Elgazery [49]. According to Hamza et al. [19] and Boussinesq's approximation, the modelled partial differential equations can be expressed in dimensional form as in Equation (1) and (2).

$$\frac{\partial u'}{\partial t'} = V_0 \frac{\partial u'}{\partial y'} + \upsilon \frac{\partial^2 u'}{\partial y'^2} + g\beta(T' - T'_m) - \frac{\sigma B_0^2 u'}{\rho} \quad (1)$$

$$\frac{\partial T'}{\partial t'} = V_0 \frac{\partial T'}{\partial y'} + \frac{1}{\rho c_p} \frac{\partial}{\partial y'}\left[k_f \frac{\partial T'}{\partial y'}\right] \quad (2)$$

The initial and boundary conditions of the current investigation are as Equation (3).

$$t' \le 0: u' = \Gamma \frac{\partial u'}{\partial y'}, T' = T'_m, \text{for } 0 \le y' \le H$$
$$t' > 0: u' \Gamma \frac{\partial u'}{\partial y'}, T' = T'_h, \text{at } y' = 0, u' = 0, T' = T'_c, \text{at } y' = H \quad (3)$$

To resolve Equation (1) to (3), we apply the nondimensional variables as in Equation (4).

$$y = \frac{y'}{H}, t = \frac{t'v}{H^2}, U \frac{u'v}{g\beta(T'_h - T'_m)H^2}$$
$$M^2 = \frac{\sigma B_0^2 H^2}{\nu\rho}, S = \frac{V_0 L}{v},$$

$$Pr = \frac{v\rho c_p}{k_m}, \theta = \frac{T' - T_m'}{T_h' - T_m'},$$
$$R = \frac{T_c' - T_m'}{T_h' - T_m'}, \lambda = \delta\left(T_h' - T_m'\right) \quad (4)$$

By using Equation (4) on Equations (1) to (3), the yield as Equation (5) and (6).

$$\frac{\partial U}{\partial t} - S\frac{\partial u}{\partial y} = \frac{\partial^2 U}{\partial y^2} - M^2 U + \theta \quad (5)$$

$$Pr\left[\frac{\partial \theta}{\partial t} - S\frac{\partial \theta}{\partial y}\right] = (1 + \lambda\theta)\frac{\partial^2 \theta}{\partial y^2} + \lambda\left[\frac{\partial \theta}{\partial y}\right]^2 \quad (6)$$

The initial and boundary conditions in the dimensionless form are shown in Equation (7).

t<0: $U = \Gamma\frac{\partial U}{\partial y}$, $\theta = 0$, $0 < y < 1$

t>0: (0) = $\Gamma\frac{\partial U}{\partial y}$, θ (0) = 1

(1) = 0 , θ(1)=R (7)

III. Method of Solution

A. Regular Perturbation Method

The approximations played an important role in the validation and study of computational solutions to challenging problems. Due to the non-linearity of this problem, we transform the governing equations into a state that can be determined analytically. Substituting $\partial u/\partial t$ = 0, and $\partial\theta/\partial t$ = 0 into Equation (5) and (6), we get Equation (8) and (9).

$$\frac{d^2 U}{dy^2} + S\frac{dU}{dy} - M^2 U = -\theta \quad (8)$$

$$(1 + \lambda\theta)\frac{d^2\theta}{dy^2} + S\,Pr\frac{d\theta}{dy} + \lambda\left[\frac{d\theta}{dy}\right]^2 = 0 \quad (9)$$

The boundary conditions are as Equation (10). We used a regular perturbation technique in the variable thermal conductivity parameter λ to create an approximate solution to Equation (8) and Equation (9) restricted to Equation (10).

(0) = $\Gamma\frac{\partial U}{\partial y}$, θ (0)= 1

(1) = 0 , θ(1)=R (10)

$$\left.\begin{aligned}\theta &= \theta_0 + \lambda\theta_1 \\ U &= U_0 + \lambda U_1\end{aligned}\right\} \quad (11)$$

By inserting Equation (11) into Equation (8) to (10), the solutions of the velocity and temperature are derived as in Equation (12) and (13).

$$\theta = A + Be^{-S\,Pr\,y} + \lambda[C + De^{-S\,Pr\,y} + ABS\,Pr\,y\,e^{-S\,Pr\,y} - B^2 e^{-2S\,Pr\,y}] \quad (12)$$

$$U = Ee^{r1y} + Fe^{-r2y} + G + He^{-S\,Pr\,y} + \lambda\begin{bmatrix} Ie^{r1y} + Je^{-r2y} + K + \\ Le^{-S\,Pr\,y} + Qye^{-S\,Pr\,y} \\ +Ne^{-2S\,Pr\,y}\end{bmatrix} \quad (13)$$

The Nusselt number and skin friction have been calculated as Equation (14) to (17).

$$\left.\frac{d\theta}{dy}\right|_{y=0} = -BS\,Pr + \lambda[-DS\,Pr + ABSPr + 2B^2] \quad (14)$$

$$\left.\frac{d\theta}{dy}\right|_{y=1} = -BSPre^{-SPr} + \lambda[-DSPre^{-SPr} + ABSPre^{-SPr} - AB(SPr)^2e^{-SPr} + 2B^2e^{-2SPr}] \quad (15)$$

$$\left.\frac{dU}{dy}\right|_{y=0} = r1E - r2F - HSPr + \lambda[r1I - r2J - LS\,Pr + Q - 2SPr] \quad (16)$$

$$\left.\frac{dU}{dy}\right|_{y=1} = r1Ee^{r1} - r2Fe^{-r2} - HS\,Pr\,e^{-SPr} + \lambda[r1Ie^{r1} - r2Je^{-r2} - LSPre^{-SPr} + Qe^{-SPr} - QSPre^{-SPr} - 2SPre^{-2SPr}] \quad (17)$$

The constants used are all indicated in the appendix section.

B. Numerical Solution

The semi-implicit finite difference approach is employed for the numerical solution of the time dependent equations as in Equations (5) to (7). The forward difference formulas were applied to all time derivatives, and the central difference formula was used to approximate the spatial derivatives. The semi-implicit finite difference equations associated with Equations (5) to (7) as in Equation (18) and (19).

$$-r1U_{j-1}^{i+1} + [1 + 2r1]U_j^{i+1} - r1U_{j+1}^{i+1} = [1 - M^2\Delta t]U_j^i + r2\left[U_{j+1}^i - U_{j-1}^i\right] + \Delta t\theta_j^i \quad (18)$$

$$-r\theta_{j-1}^{i+1} + [Pr + 2r]\theta_j^{i+1} - r\theta_{j+1}^{i+1} = Pr\,\theta_j^i + r2\,Pr\left[\theta_{j+1}^i - \theta_{j-1}^i\right] + r3\left[\theta_{j+1}^i - \theta_{j-1}^i\right]^2 \quad (19)$$

The boundary condition as in Equation (20).

$$\left.\begin{aligned} U_j^i &= \Gamma\left[\frac{U_{j+1}^i - U_{j-1}^i}{2\Delta y}\right], \\ \theta_j^i &= 1, y = 0 \\ U_N^i &= 0, \theta_N^i = R, y = 1 \end{aligned}\right\} \quad (20)$$

where,

$$r = \frac{\Delta t\left(1 + \lambda\theta_j^i\right)}{(\Delta y)^2}, r1 = \frac{\Delta t}{(\Delta y)^2}, \quad r2 = \frac{S\Delta t}{2\Delta y}, r3 = \frac{\lambda\Delta t}{4(\Delta y)^2}$$

The semi-implicit finite difference scheme is unconditionally stable (works for any time step size) and convergent. See Makinde and Chinyoka [50].

IV. Results and Discussion

The suction/injection parameter (S), slip flow parameter (Γ), Prandtl number (Pr), the magnetic number (M), the variable thermal conductivity parameter (λ), and the buoyancy force distribution parameter (R) are the non-dimensional parameters that control the flow configuration. The analytical and numerical results for momentum, energy, frictional factor, and heat transfer rate for major pertinent parameters dictating the flow are presented graphically. To ascertain the precision and correctness of the numerical approach, the approximate solutions described in the previous section are used. The numerical findings for momentum and energy are compared to the approximations to ensure the accuracy of the system. It is interesting to report that the numerical results of the momentum and energy distributions derived in Equations (12) and (13) agree well with the numerical values of the velocity and temperature deduced from Equation (18) at the unsteady state time as depicted in Figure 2. Further, Figure 3 showcases the relationship between the work of Hamza et al. [19] and the current work when S = 0 and Γ = 0. The comparison portrays an excellent relationship at steady state time.

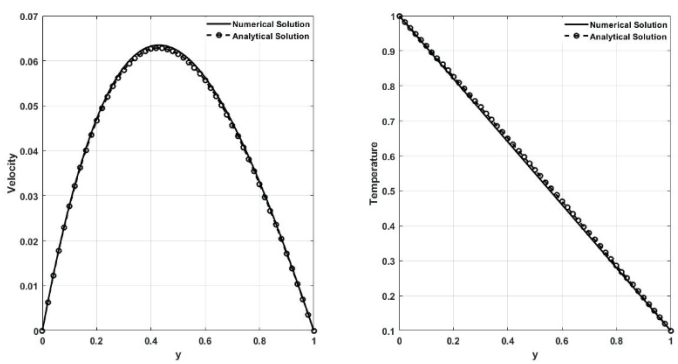

(a) Velocity (b) Temperature gradients

Figure 2: Graphs of numerical solutions and approximate solutions

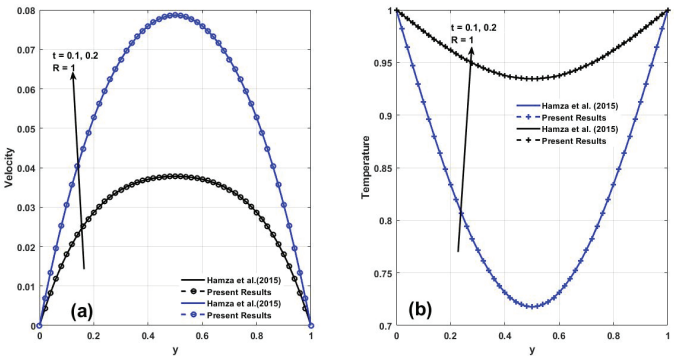

Figure 3: Comparison of [19] with the present results for the numerical solutions and the approximated solutions at R=1, t=0.1 and 0.2

The functions of the suction and injection parameters (S) and the dimensionless time (t) on the temperature and velocity distributions for the cases (i.e. R = 0 and R = 1), respectively, are shown in Figures 4 and Figure 5. It is evident that increasing the injection parameter S is seen to drastically improve the fluid velocity while raising the suction parameter is observed to produce the opposite effect. Additionally, the impact of varying thermal property parameter (λ) and time(t) for the both cases for temperature and velocity profiles is noticed to be strengthened until a steady-state time is attained. This is understandable since increasing values improves the energy difference between the outer region of the plate and the surrounding of the boundary layer according to the relationship $\lambda = \delta\left(T_h^{'} - T_m^{'}\right)$. According to Elbarbary and Elgazery [49], this results in heat moving swiftly from a plate to a liquid inside the boundary layer. Because of this, the gradients of both momentum and energy increased. It implies that as λ grows, so do the fluid flow and the thermal boundary layer thickness.

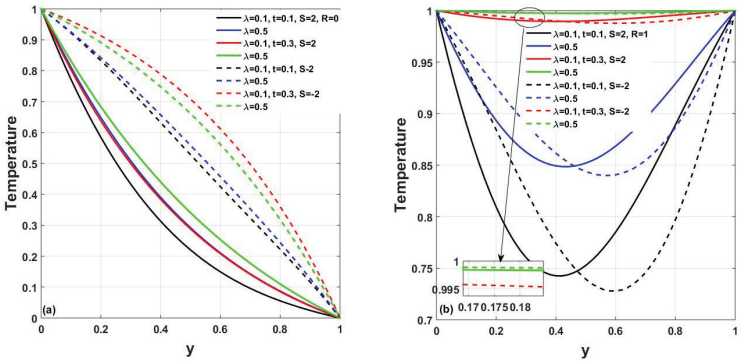

(a) R=0 (b) R=1

Figure 4: Impact of varying S, λ and t on unsteady temperature gradient

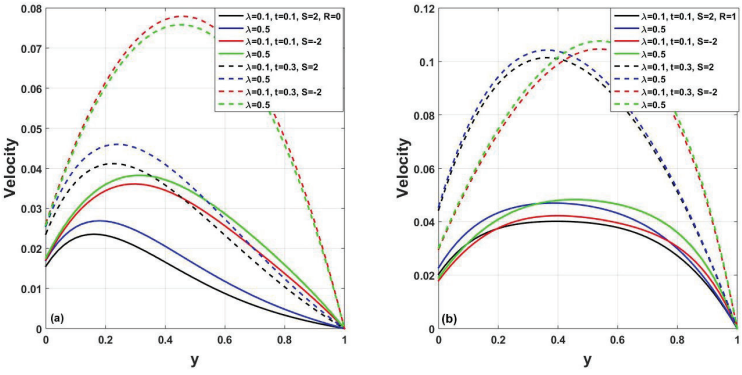

(a) R=0 (b) R=1

Figure 5: Impact of varying S, λ and t on unsteady velocity gradient for constant value of Γ

Figure 6 shows the pattern of fluid motion for varying values of the magnetic parameter (M) and non-dimensional time (t) on the temperature and velocity distributions for the asymmetric and symmetric cases. According to Figure 6 (a), the fluid velocity is highest in the region near the heated wall (y=0) and steadily weakens as it flows towards the cold plate (y=1). Figure 6 makes it evident that for all considered values of M, there is a symmetrical flow between the walls and that the figures have a parabolic shape. Additionally, it is obvious that rising values of M oppose the flow velocity along the channel surfaces in Figure 6. The availability of a magnetic effect creates a

resistivity force (the Lorentz force) that restrains velocity and is the fundamental cause of this behaviour.

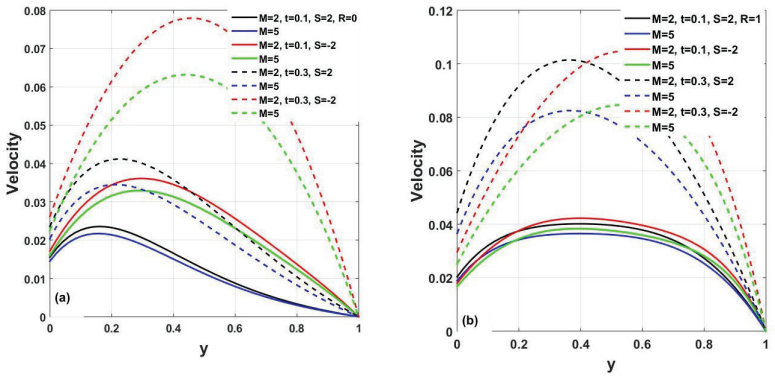

(a) R=0 (b) R=1

Figure 6: Impact of varying S, M and t on unsteady velocity gradient for constant values of Pr and Γ at (a) R=0 and (b) R=1

Figure 7 decribes the response of the suction/injection parameter (S) on the variable thermal conductivity λ to the heat transfer rate for non-dimensional time in asymmetric and symmetric cases. It can be seen from the figures that increasing the injection parameter and time t weakens the heat transfer rate at the plate (y = 0), while at higher values of the suction parameters, in both cases, an inverse effect occurs until a steady state is reached.

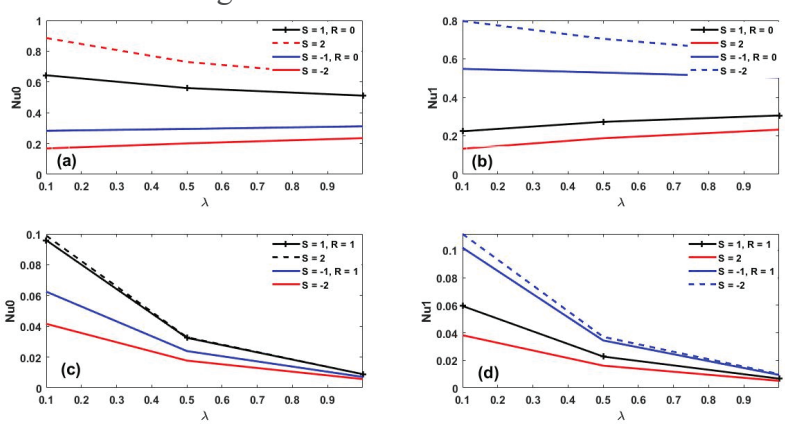

Figure 7: Deviation of unsteady and steady state Nusselt number versus λ for varying values of S and R at y=0 and y=1

Similarly, the implications of varying the suction/injection parameter (S) versus λ on the skin friction are showcased in Figures 8 for a non-dimensional time at R = 0 and R = 1, respectively. As expected, there is a stronger frictional force as the suction parameter and time are increased. However, a contrast behavior is established for rising values of the injection factor.

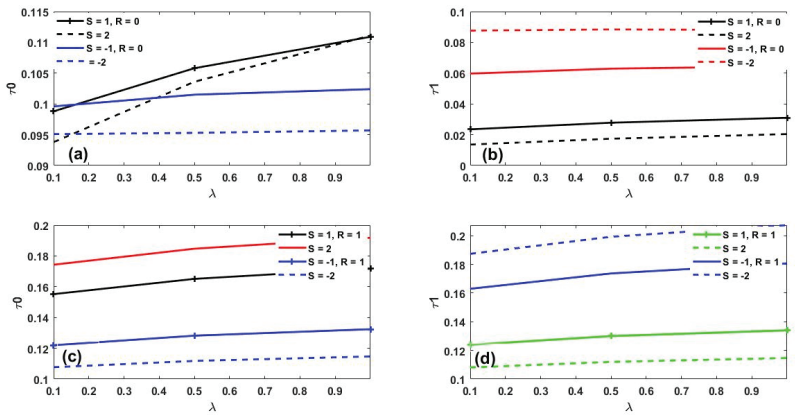

Figure 8: Deviation of unsteady and steady state Skin friction versus λ for varying values of S and R at y=0 and y=1

The sheer stress response in favor of magnetic parameter for ascending values of time at the plates y=0 and y=1 is elucidated in Figure 9 for R=0 and R=1. These figures portray that the drag force diminishes as M and t grow in asymmetric cases, as shown in Figure 9(a) and (b). Figure 9(c) and (d) are sketched to illustrate the actions of M on the drag force at both plates for R=1. It is noticeable that the skin friction decays as M grows.

The function of the velocity slip effect on the frictional factor for changing values of t at the plates y=0 and y=1 is plotted in Figure 10 for R=0 and R=1. It is clear from these figures that an escalation in the frictional factor is envisaged at both channel plates as γ and t increase for both asymmetric and symmetric cases.

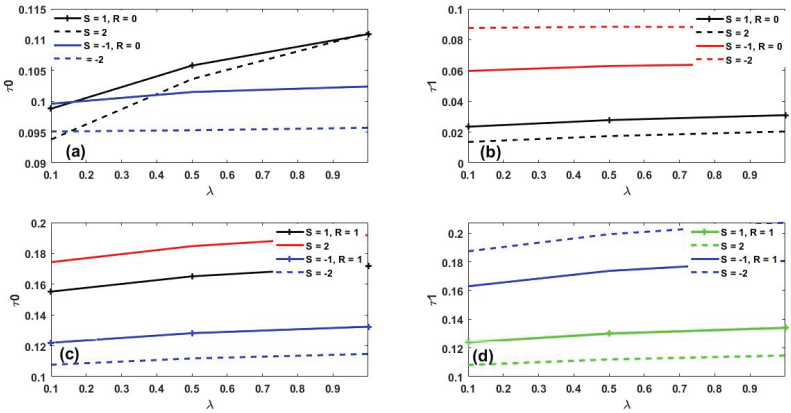

Figure 9: Deviation of unsteady and steady state Skin friction against M for different values of t and R at y=0 and y=1

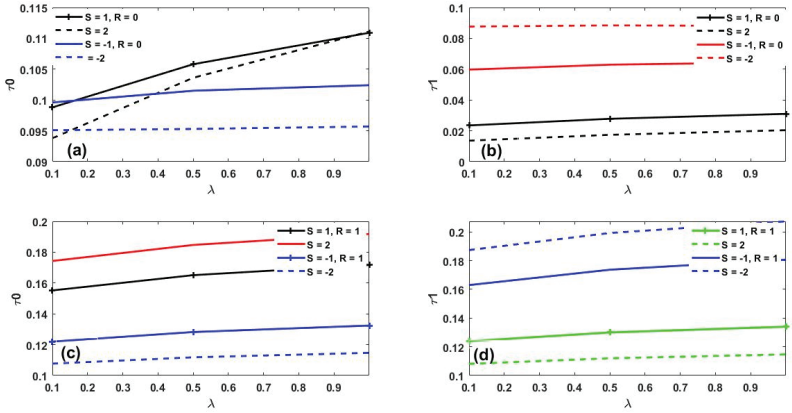

Figure 10: Deviation of unsteady and steady state Skin friction versus γ for varying values of t and R at y=0 and y=1

V. Conclusions

The analysis of unsteady and steady hydro-magnetic free convection of an incompressible and electrically conductive fluid flowing through two upright plates with asymmetric and symmetric temperatures on the channel's surface in the coexistence of suction/injection and slip effects has been investigated with the involvement of thermal property and a uniformly imposed magnetic field. The approximate and numerical solutions of the formulated partial differential equations have been derived employing the regular perturbation technique and the

semi-implicit finite difference scheme, respectively. The highlights of the key findings are summarized below:

i. The thermal and velocity flow gradients are seen to be opposed/encouraged for mounting values of suction/injection and nondimensional time for both asymmetric and symmetric cases.
ii. It is revealed that fluid motion and temperature are encouraged with mounting levels of thermal property and nondimensional time for both asymmetric and symmetric heating conditions.
iii. Uplifting the magnetic number lowers the fluid motion, but raising the nondimensional time encourages the velocity for both R = 0 and R = 1.
iv. The heat transfer amount and sheer stress are discovered to be boosted for growing values of the injection parameter at the plate (y = 0), but the converse behavior occurs at y =1 when fluid suction is raised.
v. Skin friction is a growing function of the slip parameter at both plates due to symmetric heating conditions.
vi. In the future, this work will be extended to consider the effects of porous medium and mixed convection.

VI. Appendix

$$A = 1 - \frac{R-1}{e^{-S\,\mathrm{Pr}} - 1}, \qquad B = \frac{R-1}{e^{-S\,\mathrm{Pr}} - 1},$$

$$C = B^2 - D, D = \frac{B^2 e^{-2S\,\mathrm{Pr}} - ABS\,\mathrm{Pr}\, e^{-S\,\mathrm{Pr}} - B^2}{e^{-S\,\mathrm{Pr}} - 1}$$

$$r1 = \frac{-S + \sqrt{S^2 + 4M^2}}{2}, r2 = \frac{S + \sqrt{S^2 + 4M^2}}{2},$$

$$H = \frac{-B}{\left[S\,\mathrm{Pr}^2 - S^2\,\mathrm{Pr} - M^2\right]}, \qquad G = \frac{A}{M^2}$$

$$s1 = 1 - \Gamma r1, \quad s2 = 1 + \Gamma r2, \quad s3 = Es1 + Fs2,$$

$$E = \frac{-s3e^{-r1} - s2G - s2He^{-S\,\mathrm{Pr}}}{s2e^{r1} - s1e^{-r2}}$$

$$F = \frac{s3 - Es1}{s2}, \quad K = \frac{C}{M^2},$$

$$J = \frac{p3 - Ip1}{p2}$$

$$L = \frac{-D}{S\,\mathrm{Pr}^2 - S^2\,\mathrm{Pr} - M^2},$$

$$Q = \frac{-ABS\,\mathrm{Pr}}{\left[S\,\mathrm{Pr}^2 - S^2\,\mathrm{Pr} - M^2\right]}$$

$$N = \frac{B^2}{4S\,\mathrm{Pr}^2 - 2S^2\,\mathrm{Pr} - M^2},$$

$$p1 = 1 - \Gamma r1, \quad p2 = 1 + \Gamma r2,$$

$$p3 = -K - L - N - L\Gamma S\,\mathrm{Pr} + \Gamma Q - 2\Gamma S\,\mathrm{Pr}\, N$$

$$I = \frac{-p3e^{-r2} - p2N - p2Le^{-S\,\mathrm{Pr}} - p2Qe^{-2S\,\mathrm{Pr}}}{p2e^{r1} - p1e^{-r2}},$$

B_o = Magnetic flux density [kg/s^2.m^2]

g	=	Force due to gravity [m/s^2]
H	=	Width of the channel [m]
C_pC_v	=	Specific heats at constant pressure and constant volume [$Jkg^{-1}K^{-1}$]
λ	=	Dimensionless variable thermal conductivity
R	=	Buoyancy force parameter
Γ	=	Slip flow parameter
K	=	Darcy number
Gre	=	Mixed convection parameter
γ	=	Pressure gradient
M	=	Magnetic field
S	=	Suction/injection parameter
Pr	=	Prandlt number
Nu	=	Heat transfer rate (non-dimensional)
T	=	Temperature of the fluid (non-dimensional) [K]
T_0	=	Reference temperature [K]
T^*_∞	=	The temperature far away from the plate K
U	=	Velocity of the fluid (non-dimensional) [ms^{-1}]
y	=	Distance between plates
U_0	=	Reference velocity [ms^{-1}]
β	=	Coefficient of thermal expansion [K^{-1}]
μ	=	Variable fluid viscosity [$kgm^{-1}s^{-1}$]
k	=	Thermal conductivity [$m.kg/s^3.K$]
α	=	Diffusivity of the Thermal gradient [m^2s^{-1}]
σ	=	Fluid's electrical conductivity [s^3m^2/kg]
ρ	=	Fluid density [kgm^{-3}]
v		Kinematic viscosity of the fluid[m^2s^{-1}]
α	=	Diffusivity of the Thermal gradient [m^2s^{-1}]

VII. Acknowledgement

The first author conceptualized the problem and provided the methodology. The second author contributed to the computational analysis and editing of the manuscript. The third author wrote the main draft of the manuscript, did validation and editing of the work. All the authors read and approved the final manuscript.

VIII. References

[1] M. Jawad, A. Saeed and T. Gul, "Entropy generation for MHD Maxwell nanofluid flow past a porous and stretching surface with Dufour and Soret effects", *Braz. J. Phys,* pp. 1-13. 2021. htttps://doi.org/10.1007/s13538-020-00835

[2] J. Hartmann and F. Lazarus, "Hg-dynamics II: theory of laminar flow of electrically conductive liquids in a homogeneous magnetic field", *Matematisk-Fysiske Meddelelser*, 15(7), 1937.

[3] G. Ojemeri and I. O. Onwubuya, "Significance of viscous dissipation and porosity effects in a heated superhydrophobic microchannel", *Journal of Engineering and Technology (JET),* 14(2), pp. 1-19. 2023.

[4] I. O. Onwubuya and G. Ojemeri, "Evaluation of mixed convection-radiation flow of a viscous fluid restricted to a vertical porous

channel: A comparative Study", *Caliphate Journal Science and Technology,* 5(3), pp. 1-9. 2023.

[5] M. M. Hamza G. Ojemeri and S. K. Ahmad, "Insights into an analytical simulation of a natural convection flow controlled by Arrhenius kinetics in a micro-channel", *Heliyon* 9(2023) e17628, pp. 1-13, 2023.

[6] B. K. Jha, M. M. Altine, and A. M. Hussaini, "MHD steady natural convection in a vertical porous channel in the presence of point/line heat source/sink: An exact solution", *Heat Transfer, Wiley*, pp. 1-15, 2023. DOI: 101002/htj.22903

[7] B. K. Jha, K. S. Ahmad and A. O. Ajibade, "Unsteady/steady free convective Couette flow of reactive viscous fluid in a vertical channel formed by two vertical porous plates", *Int. Sch Res. Net., ISRN therm.*, 2012. DOI:10.5402/2012/794741

[8] A. Saeed and T. Gul, "Bio-convection Casson nano-fluid flow together with Darcy-Forchheimer due to a rotating disk with thermal radiation and Arrhenius activation energy", *SN Applied Science*, 3, 78,2021.

[9] J. V. R. Reddy, K. A. Kumar, V. Sugunamma and N. Sandeep, "Effect of cross diffusion on MHD non-Newtonian fluids flow past a stretching sheet with non-uniform heat source/sink: A comparative study", *Alexandria Eng. J.* 57(3), pp. 1829–1838, 2018.

[10] C. S. Sravanthi and R. S. R. Gorla, "Effects of heat source/sink and chemical reaction on MHD Maxwell nanofluid flow over a convectively heated exponentially stretching sheet using Homotopy analysis method", *Int. J. Appl. Mech. Eng.* 23(1), pp. 137–159, 2018.

[11] P. Gurivireddy, M. C. Raju, B. Mamatha, S. K. Varma, "Thermal diffusion effect on MHD heat and mass transfer flow past a semi-infinite moving vertical porous plate with generation and chemical reaction", *Applied Mathematics,* 7 (7), 638, 2016.

[12] G. Ojemeri, E. Omokhuale, M. M. Hamza, I. O. Onwubuya and A. Shuaibu, "A Computational Analysis on Steady MHD Casson Fluid Flow Across a Vertical Porous Channel Affected by Thermal Radiation Effect", *Int. J Sci Glob Sus.,* **9**(1) (2023). https://doi.org/ 10.57233/ijsgs.v9i1.393

[13] M. M. Hamza, A. Shuaibu and S. K. Ahmad, Unsteady MHD free convection flow of an exothermic fluid in a convectively heated vertical channel filled with porous medium", Scientific Reports, 12, 11989, 2022.

[14] A. M. Obalalu, O. A. Ajala, A. T. Adeosun, A. O. Akindele, O. A. Oladapo and O. A. Olajide, "Significance of variable electrical conductivity on non-Newtonian fluid flow between

two vertical plates in the coexistence of Arrhenius energy and exothermic chemical reaction", *Partial Diff. Eqn Appl Math,* 4, 100184, pp. 1-9, 2021.

[15] G. Ojemeri and M. M. Hamza, "Heat transfer analysis of Arrhenius-controlled free convective hydromagnetic flow with heat generation/absorption effect in a micro-channel", *Alexandria Eng. J.*, 61, pp. 12797-12811, 2022.

[16] M. M. Hamza, I. Bello, A. Mustapha, U. Usman and G. Ojemeri, "Determining the role of thermal radiation on hydro-magnetic flow in a vertical porous superhydrophobic microchannel", *Dutse J. Pure Applied Sci,* 9(2b), pp. 297-308, 2023.

[17] A. O. Ajibade and T. M. Kabir, "The Combined Effect of Variable Viscosity and Variable Thermal Conductivity on Natural Convection Couette Flow. International Journal of Thermofluids". (2020). https://doi.org/10.1016/j.ijft.2020.100036

[18] O. Salawu, S. S. Okoya and A. R. Hassan, "On free convection flow of a moving vertical permeable plate with quadratic Boussinesq approximation and variable thermal conductivity", *Heat Transfer Research*, 52 (7), 2021.

[19] M. M. Hamza, I. G. Usman and A. Sule, "Unsteady/steady hydromagnetic convective flow between two vertical walls in the presence of variable thermal conductivity", *Journal of fluids,* volume 2015, Article ID:358053.

[20] S. Pradip, K. Sarker and Md. M. Alam, "Effect of variable viscosity and thermal conductivity on MHD natural convection flow along a vertical flat plate", *Journal of Advances in Mathematics and Computer Science,* 36 (3) pp. 58-71, 2021.

[21] M. G. Reddy, "Effects of thermophoresis, viscous dissipation and joule heating on steady MHD flow over an inclined radiative isothermal permeable surface with variable thermal conductivity", *J. Appl Fluid Mech,* **7**(1) pp. 51–61, 2014.

[22] I. L. Animasaun and N. Sandeep, Buoyancy induced model for the flow of 36 nm alumina-water nanofluid along upper horizontal surface of a paraboloid of revolution with variable thermal conductivity and viscosity", *Powder Tech*. 301, pp. 858–867, 2016.

[23] T. Salahuddin and M. A. Awais, "Comparative study of Cross and Carreau fluid models having variable fluid characteristics", *Int. Comm. Heat Mass Transf.* 139, 106431, 2022.

[24] T. Abbas, S. Rehman, R. A. Shah, M. Idrees and M. Qayyum, "Analysis of MHD Carreau fluid flow over a stretching permeable sheet with variable viscosity and

thermal conductivity", *Phys. A*, 551, 124225, 2020.

[25] M. Khan, M.Y. Malik, T. Salahuddin and I. Khan, "Numerical modeling of Carreau fluid due to variable thicked surface", *Results Physics*, 7, pp. 2384–2390. 2017.

[26] N. R. Nalivela, S. R. Vempati, R. B. Ravindra and R. Y. Dharmendar, "Viscous dissipation and thermal radiation impact on MHD mass transfer natural convective flow over a stretching sheet", *Proc. Inst. Mech. Eng. Part E J. Process Mech. Eng.* 2022.

[27] A. M. Megahed, "Carreau fluid flow due to nonlinearly stretching sheet with thermal radiation, heat flux, and variable conductivity", *Appl. Math. Mech.* 40(11), pp. 1615–1624, 2019.

[28] M. Irfan, M. Khan and W. A. Khan, "Interaction between chemical species and generalized Fourier's law on 3D flow of Carreau fluid with variable thermal conductivity and heat sink/source: A numerical approach" *Results Physics*, 10, pp. 107–117, 2018.

[29] M. Waqas, A. Alsaedi, S. A. Shehzad, T. Hayat and S. Asghar, "Mixed convective stagnation point flow of Carreau fluid with variable properties", *J. Braz. Soc. Mech. Sci. Eng.* 39(8), pp. 3005–3017, 2017.

[30] K. M. Ewis, "Effects of variable thermal conductivity and Grashof number on non-Darcian natural convection flow of viscoelastic fluids with non-linear radiation and dissipation", *J. Adv. Res. Appl. Sci. Eng. Tech.*, 22 (1), 2021.

[31] Hamza, M. M., Abdullahi, U., Ahmad, S. K., Omokhuale, E.: Mixed convection flow in a microchannel in the presence of magnetic field and thermal property, *International Journal of Science for Global Sustainability,* 8(4) (2022).

[32] G. Borah and G. C. Hazarika, "Effects of variable viscosity and thermal conductivity and magnetic field effect on the free convection and mass transfer flow through porous medium with constant suction/heat flux" *J. Comp Math. Sci*., 4(6), pp. 407-418, 2013.

[33] Md. R. Haque, Md. M. Alam, M. M. Ali and R. Karim, "Effect of viscous dissipation on natural convection flow over a sphere with temperature dependent thermal conductivity in presence of heat generation", *Proc. Eng.* 105, pp. 215-224, 2015.

[34] P. Bandita, "Effects of variable viscosity and thermal conductivity on steady MHD slip flow of micropolar fluid over a vertical plate" *Int. J. Comp. Appl. Tech. Res.*, 6(7), pp. 293-298, 2017.

[35] A. Pantokratoras, Effects of variable viscosity and thermal conductivity on steady MHD flow

of a micropolar fluid through a specially characterized horizontal channel", *Heat transfer AMSE,* 86(1), pp. 1-13, 2017.

[36] G. C. Hazarika and B. Phukan, "Effect of viscous dissipation in natural convection along a heated vertical plate" *Appl Math Mod.* 29, pp. 553-564, 2005.

[37] A. K. Mishra, T. Paul and A. K. Singh, "Mixed convention flow in a porous medium bounded by two vertical walls", *Forsch Ingenieurwes,* 67, 198–205, 2022.

[38] R. C. Chaudhary and A. Jain, "Combined heat and mass transfer effects on MHD free convection flow past an oscillating plate embedded in porous medium" *Romania Journal of Physics,* 52, pp. 505–524, 2007.

[39] A. Khalid, I. Khan and A. Khan, "Unsteady MHD free convection flow of Casson fluid past over an oscillating vertical plate embedded in a porous medium" *Engineering Sciences and Technology*, 18, 309–317, 2015.

[40] B. K. Jha, M. M. Altine and A. M. Hussaini, "Role of suction/injection on free convective flow in a vertical channel in the presence of point/line heat source/sink", *ASME Journal of Heat Transfer*, 144, 062602, 2022.

[41] I. J. Uwanta and M. M. Hamza, "Effect of Suction/Injection on Unsteady hydro-magnetic Convective Flow of Reactive Viscous Fluid Between Vertical Porous Plates with Thermal Diffusion", *International Scholarly Research,* Article ID 980270, 1–14, 2014.

[42] B. K. Jha, B. Y. Isah, and I. J. Uwanta, "Combined Effect of Suction/Injection on MHD Free-Convection Flow in a Vertical Channel with Thermal Radiation", *Ain Shams Engineering Journal*, 9(4), 1069–1088, 2018.

[43] B. K. Jha, L. A. Azeez, and M. O. Oni, "Unsteady Hydromagnetic-Free convection flow with suction/injection", *Journal of Taibah University*, 13, 136–145, 2019.

[44] N. I. Kamis, Md. F. Bashir, S. Shafie, T. K. A. Khairuddin and L. Y. Jiann. "Suction effect on an unsteady Casson hybrid nanofluid film past a stretching sheet with heat transfer analysis", *IOP Conferenece Series: Materials Science and Engineering,* 1078, 2021.

[45] N. I. Kamis, N. A. Rawi, L. Y. Jiann, S. Shafie and M. R. Ilias, "Thermal characteristics of an unsteady hybrid nano-Casson fluid passing through a stretching thin-film with mass transition" *Journal of Advance Research in Fluid Mechanics and Thermal Sciences,* 104(2), 2023.

[46] N. I. Kamis, L. Y. Jiann, S. Shafie, T. K. A. Khairuddin and Md. B. Faisal,

"Magnetohydrodynamics boundary layer flow of hybrid nanofluid in a thin film over an unsteady stretching permeable sheet" *Journal of Nanofluid,* 11(1), 74-83, 2022.

[47] N. Bachok, S. N. N. Tajuddin, N. S. Anuar, and H. Rosali, "Numerical computation of stagnation point flow and heat transfer over a nonlinear stretching/shrinking sheet in hybrid nanofluid with suction/injection effects" *Journal of Advance Research in Fluid Mechanics and Thermal Sciences,* 107(1), 2023.

[48] S. H. H. Karouei, M. B. Shani, M. Sekaloo, S. H. H. Eimeni, P. Pasha, D. D. Ganji "Computational modelling of magnetized hybrid nanofluid flow and heat transfer between parallel surfaces with suction/injection", *International Journal of Thermofluids,* 22, 100613, 2024.

[49] E. M. E. Elbarbary and Elgazery, "Chebyshev finite difference method for the effects of variable viscosity and variable thermal conductivity on heat transfer from moving surfaces with radiation", *Int. J. Ther Sci,* 43(9), pp.889–899, 2004.

[50] O. D. Makinde and T. Chinyoka, "Numerical study of unsteady hydromagnetic Generalized Couette flow of are active third-grade fluid with asymmetric convective cooling", *Computers and Mathematics with Applications*, 61, pp.1167-1179, 2011.